Hindawi
Advances in Multimedia
Volume 2021, Article ID 3955316, 9 pages
https://doi.org/10.1155/2021/3955316

Research Article

Art Online Design Based on Digital Simulation Technology

Song Gao

Xinyang Vocational and Technical College, Xinyang 464000, China

Correspondence should be addressed to Song Gao; ys059@xyvtc.edu.cn

Received 15 October 2021; Revised 3 November 2021; Accepted 18 November 2021; Published 30 November 2021

Academic Editor: Qiangyi Li

In order to improve the humanization and convenience of online art design, this paper applies digital simulation technology to the art online design system and establishes a set of sequential multi-free-form surface design methods. Based on the obtained front free-form surfaces, this paper establishes the relationship between the discrete points on the subsequent free-form surfaces and their spatial solid angles and, through extremely complex theoretical deduction, finally obtains the subsequent free-form surfaces. In addition, by combining the two free-form surfaces to enter the 3D modeling software, we can obtain an optical lens with multiple free-form surfaces to improve the digital simulation effect. Finally, this paper uses the intelligent system constructed in this paper to conduct multiple sets of simulation experiments to evaluate the digital effect and artistic design effect of the system constructed in this paper. From the experimental research, it can be known that the art online design system based on digital simulation technology constructed in this paper basically meets the expected goals of the system constructed in this paper.

1. Introduction

The current era is an era of rapid and fierce competition, and competition mechanisms have penetrated into all areas of society. In this case, if its products cannot accurately and quickly adapt to the needs of the market, the outcome will be terrible. If it wants to occupy a place in the fierce market competition or to expand the industry, there is no doubt that it needs to work hard on product positioning and product artistic conception [1]. This requires product designers to integrate the artist's ideas and then design, test, modify, and complete the product. In view of the development of computer graphics and the maturity of realistic graphic design technology, we can design software [2] to realize the realistic simulation of artworks. In this way, we can immediately show the artist's idea in an intuitive form, which is convenient for the artist to repeatedly and quickly modify his artistic idea. In this way, work efficiency will be improved [3].

Based on the above analysis, this paper applies digital technology to art design and builds an art online design platform based on digital simulation technology to improve the effect of art design and at the same time improve the combination of art design and computer-aided design.

2. Related Work

Stereo vision originated in the 1960s, and it has achieved unprecedented development. Compared with photogrammetry and structured light measurement methods, stereo vision measurement is simpler and more flexible [4]. The principle is to observe the same scene from two or more viewpoints, obtain a set of images in different perspectives and the aberrations between corresponding image points in different images through the principle of triangulation, and then infer the space of the target object in the scene geometry and location [5]. Stereo vision measurement technology has been widely used in various dynamic and static measurements. The Department of Mechanical Engineering of Zhejiang University uses the principle of perspective imaging and the binocular stereo vision method to achieve dynamic and accurate position detection of multi-degree-of-freedom mechanical devices [6]. Klockars et al. [7] proposed a new method for minimizing the absolute value of gray-scale correlation multipeak disparity stereo matching, which can perform noncontact static and accurate measurement of the three-dimensional space coordinates of irregular objects. With the research on stereo vision measurement technology, in the large-scale measurement, Hermus et al. [8] adopt the

relaxation method for image matching, and the error of the image detection at 300 cm is about 2.6 cm. When the detection distance increases to 700 cm, the measurement error is about 31.9 cm. In the macromeasurement, Calvert and Schyfter [9] detect the protrusion degree of the eyeball based on the binocular stereo vision measurement method. First, by building a binocular stereo vision platform, the high-quality dataset needed for the experiment is obtained, and the method of measuring eyeball protrusion is studied, feature point matching, key point extraction, and three-dimensional reconstruction are achieved, and the measurement result of eyeball protrusion is obtained by fitting. Thus, it can be compared with the manual measurement results and the accuracy is analyzed; finally, it is concluded that the experiment can follow the in-depth study of the visual measurement. Based on the development status of visual measurement, the principle of binocular vision measurement is applied to the detection of human pulse signals to obtain dynamic three-dimensional information of human pulse to study the physiological and pathological conditions of the human body. However, there are many error factors in the process of visual measurement, which affect the accuracy of the measurement [10].

It is very important to analyze the accuracy of the binocular vision measurement system, but there are many factors that cause measurement errors. At present, many experts and scholars at home and abroad have conducted in-depth research on the error of vision measurement, for example, the resolution error of the CCD array, the matching error, and the position error between the two cameras [11]. Thorpe and Manzini [12] analyzed the matching error of the binocular system. Sclater and Lally [13] analyzed the resolution error of the CCD array. The calibration error and position error between the two cameras can be reduced by improving the experimental system, but they cannot be eliminated. Due to the existence of measurement errors, the measurement accuracy is greatly affected. Therefore, it is of great significance to analyze the error.

With its excellent measurement performance, laser displacement sensors are widely used in vibration measurement, thickness detection, and three-dimensional contour acquisition [14]. The working principle is that the laser transmitter generates a parallel beam of light, which is focused on the surface to be measured by a condensing lens, and the surface to be measured produces diffusely reflected light, and part of the light is imaged on the CCD photosensitive surface. When the measured object moves along the direction of the incident light, the position of the scattered light spot on the surface of the measured object changes on the imaging objective lens, thereby changing the position of the image point on the photosensitive device. By accurately measuring the moving distance of the image point on the photosensitive surface of the linear CCD, the displacement of the measured object can be obtained [15]. According to the position relationship between the incident light and the measured surface, the detection mode of the laser displacement sensor is divided into direct and oblique [16].

3. Digital Image Simulation Algorithm

In optical measurement, it is very difficult to accurately obtain the coordinate information of a strongly reflective surface. For the digital design of artworks, the most used method is to design artwork parameters through optical measurement, and optical measurement is based on accurately receiving image information as a prerequisite for measurement. The strong reflective surface of the object surface is presented on the image with over-saturation and over-darkness, which brings difficulties to the recognition of the details of the image, produces image distortion, and affects the measurement accuracy.

As shown in Figure 1, the reason is that there is a strong reflection area on the design plane of the artwork, which causes the uneven light to illuminate its surface and will significantly reduce the reliability of the measurement.

When the light bar is irradiated on a plane, strong reflection occurs, the light bar becomes thicker, and the center of gravity of the light bar produces high-frequency jitter and is seriously deviated from the original position, which leads to deviations in measurement and difficulty in extracting marker points. Therefore, it is not suitable for aperture measurement.

In response to this problem, many scholars at home and abroad have conducted research on the subject of eliminating the influence of strong reflective surfaces. Richard uses the different characteristics of the images formed by different angles of incident light irradiated in the strong reflection area to collect objects at different angles and then stitches the partial images. However, this method may produce errors during the splicing process, which affects the accuracy. SHINJI uses the characteristics of specular reflection and diffuses reflection in the surface structure of the measured object with different polarization characteristics to install different polarizers in front of the lens to filter out the specular reflection that affects the measurement and retains the diffuse reflection for measurement. However, the diffuse reflected light is weak and the measurement accuracy will be limited. This method retains the edge information very well, but needs to perform multilevel Canny transformation, which requires a long calculation time and low real-time performance. Combined with the above analysis, this paper decided to collect the artwork image again on the basis of the previous experiment and get the image, as shown in Figure 2.

Based on the analysis of the strong reflection around the artwork, this paper combines the existing image noise processing methods to propose an aperture measurement method based on fractional differential to remove strong local reflections. It uses fractional differentiation to process the image of the strongly reflective surface around the circular hole, which eliminates the influence of the highly reflective area on the edge of the circular hole and improves the accuracy of the experiment.

Due to the characteristics of the art design process, uneven reflection occurs when light is irradiated, and the polarization state of the reflected echo will show a different state. Moreover, its reflectance and phase angle will change irregularly, and the uneven reflection characteristics of the

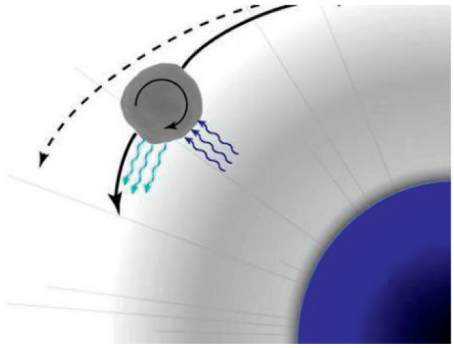

Figure 1: Schematic diagram of strong reflective surface.

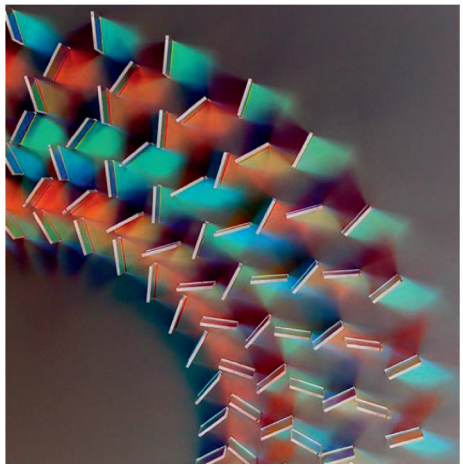

Figure 2: Schematic diagram of artwork.

strong reflection area will have unpredictable effects on its surrounding objects. The incident light has different reflection characteristics when irradiated on the surface of the object. According to the reflection characteristics of the surface of the object, the surface of the object can be divided into Lambertian surfaces, mirror surfaces, and surfaces with reflection characteristics in between, as shown in Figure 3. When incident light is projected on the surface, strong specular reflection occurs, and the intensity of the reflected light fed back from different positions on the surface is not the same.

According to Beckman's rough surface scattering theory, when the incident light hits the reflective surface, most of the incident light will follow the law of specular reflection, while a part of it will be scattered on the surface of the measured object, and a very small part of the reflected light will diverge and scatter at all angles in the space. Its strength is related to the surface roughness. The two parts of the reflected light form a scattered light spot in the space. Because the area of the CCD detection surface is limited, the CCD detection plane speckle extends from the origin of the camera center to the space. E_C represents the area of planar speckle detection:

$$E_C = \iint C_1(\Delta x, \Delta y) d\Delta x d\Delta y. \tag{1}$$

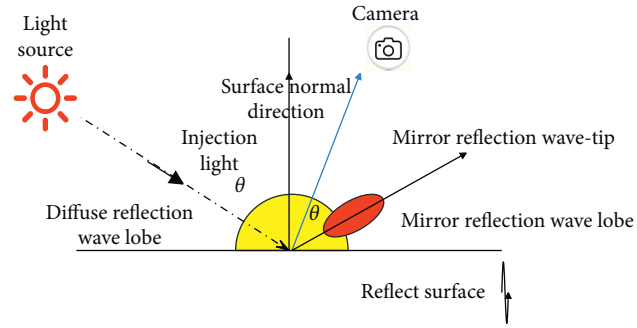

Figure 3: Basic reflection form of light.

In the formula, $C_1(\Delta x, \Delta y)$ represents the intensity of speckle. If $C_1(\Delta x, \Delta y)$ drops to $1/e$ at r_0, then the area is

$$E_C = \frac{\lambda^2 z^2}{2\pi r_0^2}. \tag{2}$$

In the formula, λ is the wavelength of incident light and z is the distance from the measured plane to the imaging plane. The area of E_C has a great restriction on the accuracy of the measurement in this paper. If $C_1(\Delta x, \Delta y)$ exceeds the resolution capability of the camera itself, this part of the image with speckle noise is difficult to be captured by the camera and presented in the image.

If you simply reduce the brightness of the light source or use a uniform illuminating light source to reduce the impact of specular reflection, the detailed information of the image may not be clearly reflected in the collected image. The result is that the accuracy is not high and does not meet the requirements of industrial production if the light-absorbing material is uniformly sprayed on the strong reflective surface. Since the objects with small apertures are collected, subtle aperture changes may cause inappropriate production of parts, increase costs, and are not suitable for use. Therefore, in order to eliminate the influence of local high-brightness areas and retain more detailed information on the aperture edge of the original image, it is necessary to suppress the strong reflection influence of the high-reflective area and eliminate or weaken the influence of the strong reflective surface on the next step, while ensuring the image quality Improve measurement accuracy.

After mathematicians discovered the limitations of integer-order differentiation, they generalized the integer-order differentiation to obtain the fractional order differentiation. In the image processing process, some noncausal, nonlinear, and other difficult-to-solve problems can be performed by fractional-order differentiation treatment and achieved good results. The purpose of image preprocessing is to improve the image quality while preserving the area of interest. This article uses image processing to correct the unevenness of the image brightness, weaken the projection of the incident light component, suppress low-frequency information, and also need to enhance the reflected light component, that is, enhance the high-frequency edge information, eliminate the influence of the strong reflection area, and completely retain the detailed information around the edge of the circular hole, so as to correct the influence of uneven brightness. Fractional

differentiation can just solve the above problem. As shown in Figure 4, comparing the amplitude-frequency characteristic curves of the fractional derivative with $v = 0.2$, $v = 0.5$, and $v = 0.7$ and the integer-order derivative with $v = 1$ and $v = 2$, it can be found that the fractional order of any order differentiation can enhance the high-frequency signal of the image. In the image processing, the edge information can be enhanced, but at the same time, the high-frequency noise can be suppressed. The preservation of faint details is something that integer-order differentiation does not have.

When using fractional differentiation to differentiate artwork images, according to the characteristics of the fractional differentiation itself, high-frequency edge information can be enhanced to improve edge extraction accuracy. At the same time, it attenuates high-frequency noise. That is, it can eliminate the influence of strong reflective areas, and it can retain weak edge information nonlinearly.

At present, there are three mainstream definitions for fractional differential: Grunwald–Letnikov definition, Riemann–Liouville definition, and Caputo definition. Since there is no uniform stipulation form, we use three aspects to explain.

3.1. Grunwald–Letnikov (G-L) Definition. According to the information, the G-L definition of the three fractional differential definitions has the best effect when processing images. The G-L fractional differential is defined as follows:

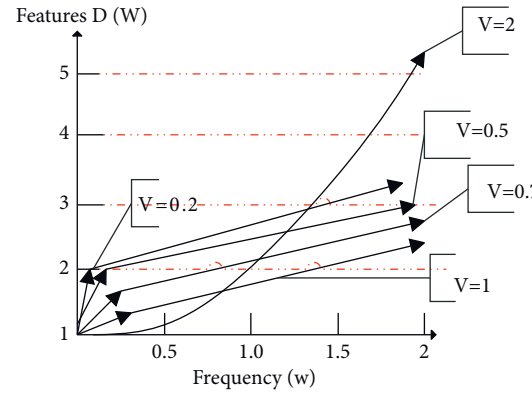

FIGURE 4: Fractional differential amplitude-frequency characteristic curve.

$$f^{(n)}(t) = \frac{d^n f}{dt^n} = \lim_{h \longrightarrow 0} h^{-n} \sum_{j=0}^{n} (-1)^j \binom{n}{j} f(t - jh). \quad (3)$$

$\forall v \in R$, and when rounding v, it is expressed as $[v]$. If the signal $f(t) \in [a, t]\,(a < t, a \in R, t \in R)$ has a continuous $m+1$ order derivative and when $v > 0$, m is at least an integer; then, the noninteger v-order derivative G-L definition expression of the signal $f(t)$ is [17]

$$\begin{aligned} {}_a^G D_t^v f(t) &\cong \lim_{h \longrightarrow 0} f_h^{(v)}(t) \cong \lim_{\substack{h \longrightarrow 0 \\ nh = t-a}} h^{-v} \sum_{j=0}^{[(t-a)/h]} (-1)^j \binom{n}{j} f(t - jh) \\ &\cong \lim_{n \longrightarrow \infty} \left\{ \frac{(t - a/n)^{-v}}{\Gamma(-v)} \sum_{j=0}^{(t-a)/(h-1)} (-1)^j \frac{\Gamma(j - v)}{\Gamma(j+1)} f\left(t - \frac{j(t-a)}{n}\right) \right\}. \end{aligned} \quad (4)$$

In the formula, the Gamma function is

$$\begin{aligned} \Gamma(n) &= \int_0^{\infty} e^{-t} t^{n-1} \mathrm{d}t = (n-1), \\ \begin{bmatrix} -v \\ r \end{bmatrix} &= \frac{(-v)(-v+1)\cdots(-v+r-1)}{r!}. \end{aligned} \quad (5)$$

In order for $f_h^{(v)}(t)$ to reach the nonzero limit, that is, $h \longrightarrow 0$, $n \longrightarrow \infty$ is required. We set $h = t - a/h$, that is, $n = t - a/h$. In mathematics, G-L definition has properties such as continuity and boundedness, but it must have a strong condition to satisfy it, that is, the order V must satisfy $m < Re(v) < m + 1$. However, this condition is not easy to satisfy, so Letnikov proposes a definition of weakening condition in order to solve this problem, which is usually called the Riemann–Liouville definition.

3.2. Riemann–Liouville (R-L) Definition

$${}_a^L D_t^v f(t) = \frac{1}{\Gamma(-v + m + 1)} \left(\frac{d}{\mathrm{d}t}\right)^{m+1} \int_a^t (t - \tau)^{m-v} f(\tau) \mathrm{d}\tau. \quad (6)$$

The condition of this formula is that when $t \in (a, +\infty)$, $f(t)$ is continuous in this interval, and when $t = a$, $f(t)$ is infinite. However, although this definition has theoretical meaning, it has no physical meaning. Therefore, in 1967, M. Caputo proposed an integer-order Caputo definition that can only calculate the initial value of the derivative function.

3.3. Integer-Order Caputo Definition

$${}_a^C D_t^v f(t) = \frac{1}{\Gamma(n - v)} \int_a^t \frac{f^{(n)}(\tau) \mathrm{d}\tau}{(t - \tau)^{v+1-n}}, \; (n - 1 < v < n). \quad (7)$$

Formulas (4), (6), and (7) are three different definitions of fractional differentiation given by different mathematicians from different angles. Under certain conditions, they are mutual improvements to the former definition, but they restrict each other. These three definitions can be converted mutually under certain conditions.

In advanced mathematics, the derivative of a point in its neighborhood is the derivative of that point, and the derivative of this point can be used to detect and process the instantaneous signal at this time. When the differential order is a fraction, $h^v > h$, which is manifested in the image which is to enlarge the sampling interval. This means that the quality of image processing is improved.

The properties of fractional differentials can be summarized as continuity, nonlinearity, and value constancy.

3.3.1. Continuity. Because of $\lim_{v_1 \to v_2} D^{v_1} f(t) = D^{v_2} f(t)$, it can be seen that the fractional differential has continuity. Intuitively, when two infinitely close fractional differentials are calculated separately, the results of the calculations are also infinitely similar. At the image processing level, when the fractional order is selected close, the effect of the two processing is also very close. Because the integer is extended to a wider fractional level, the fractional differential has a wider application range.

3.3.2. Nonlinearity. The correspondence between $f(t)$ and $D^v f(t)$ is nonlinearity. In real life, most things are nonlinear relations, and linear relations are only in an ideal state. Therefore, when we use nonlinear fractional differentiation to process images, we may unexpectedly obtain better results.

3.3.3. Value Constancy. Similar to the nature of the power function, when a signal occurs, the phase response of the fractional derivative is a constant value, and the amplitude response is different from the integer-order derivative. For any image, we define its signal as $f(t) \in L^2(R)$ and perform Fourier transform on $f(t)$ [18]:

$$\widehat{f}(\omega) = \int_R f(t) \cdot e^{-i\omega t} \mathrm{d}t. \tag{8}$$

By performing kth order differential operation on $f(t)$, the Fourier transform of $f^{(k)}(t) = D_k f(t) = d^k f(t)/\mathrm{d}t^k$ is obtained as [19]

$$\left(D_k, \widehat{f}\right)(\omega) = (i\omega)^k \widehat{f}(\omega) = \widehat{d}_k(\omega) \cdot \widehat{f}(\omega), \tag{9}$$

where $(i\omega)^k = \widehat{d}(\omega)$ is the kth order differential multiplier function, where the exponential function of $\widehat{d}(\omega)$ is

$$\begin{cases} \widehat{d}_k(\omega) = \widehat{a}_k(\omega) \cdot \exp\left[i\theta_k(\omega)\right] \\ \widehat{a}_k(\omega) = |\omega|^k, \theta_k(\omega) = \dfrac{k\pi}{2}\operatorname{sgn}(\omega) \end{cases}, \quad k \in Z^+. \tag{10}$$

By extending formula (10) to any order operator D_v, the frequency domain of the derivative $f^{(v)}(t)$ of the fractional differential can be obtained as

$$\left(D_v, \widehat{f}\right)(\omega) = (i\omega)^v \widehat{f}(\omega) = \widehat{d}(\omega) \cdot \widehat{f}(\omega). \tag{11}$$

Among them, the exponential form of $\widehat{d}(\omega)$ is [20]

$$\begin{cases} \widehat{d}_v(\omega) = \widehat{a}_v(\omega) \cdot \exp\left[i\theta_v(\omega)\right], \\ \widehat{a}_v(\omega) = |\omega|^k, \theta_v(\omega) = \dfrac{k\pi}{2}\operatorname{sgn}(\omega). \end{cases} \tag{12}$$

For a two-dimensional image $f(x, y)$, $f(x, y)$ performs fractional differentiation on the (x, y) coordinate axis in the x and y directions to obtain partial derivatives, and the approximate expression can be obtained as

$$\begin{aligned} \frac{\partial^v f(x,y)}{\partial x^v} &\approx f(x,y) - vf(x-1,y) + \frac{v(-v+1)}{2} f(x-2,y) \\ &\quad + \cdots + \frac{\Gamma(-v+1)}{n!\Gamma(-v+n-1)} f(x-n,y), \\ \frac{\partial^v f(x,y)}{\partial x^v} &\approx f(x,y) - vf(x-1,y) + \frac{v(-v+1)}{2} f(x,y-2) \\ &\quad + \cdots + \frac{\Gamma(-v+1)}{n!\Gamma(-v+n-1)} f(x,y-n). \end{aligned} \tag{13}$$

The coefficient of the first $n+1$ term in the above formula is [21]

$$\begin{cases} a_0 = 1, a_1 = -v, a_2 = \dfrac{(-v)(-v+1)}{2}, \\ a_3 = \dfrac{(-v)(-v+1)(-v+2)}{6}, \\ a_n = \dfrac{\Gamma(-v+1)}{n!\Gamma(-v+n+1)}. \end{cases} \tag{14}$$

For an image in the form of $M \times N$, if you want to process the image completely, you must take $g(x, y)$ as the center and perform fractional differentiation in 8 directions in sequence. Figure 5 is a schematic diagram of the direction of fractional differential operation.

From the schematic diagram of the direction of the fractional differential operation, it can be seen that the operator has a high degree of symmetry. Due to the complex features of the artwork, in order to achieve the effect of enhancing the edge contour of the circular hole while weakening the influence of the strong reflective surface, the strong reflection area around the artwork can be suppressed and eliminated, and the edge of the circular hole must be completely preserved. Compared with the above analysis of the definition and properties of the fractional differential, combined with the fractional differential on the high-brightness area of the strong reflective area, frequency noise

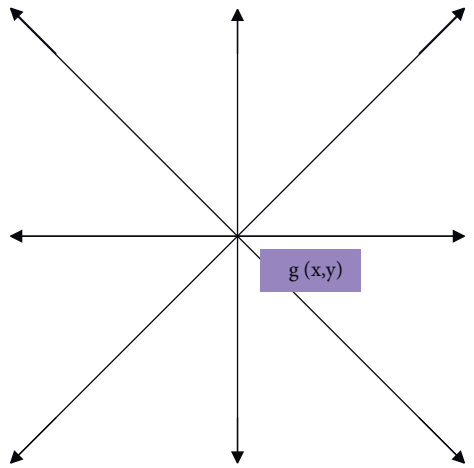

Figure 5: Schematic diagram of the direction of fractional differential operation.

has a good suppression effect and can improve the accuracy of edge extraction. It is decided to use a fractional differential operator to process the original image of the collected artwork, using a 5* 5 template, as shown in the following formula [22]:

$$W_{5*5} = \begin{bmatrix} a_2 & 0 & a_2 & 0 & a_2 \\ 0 & a_1 & a_1 & a_1 & 0 \\ a_2 & a_1 & 8 * a_0 & a_1 & a_2 \\ 0 & a_1 & a_1 & a_1 & 0 \\ a_2 & 0 & a_2 & 0 & a_2 \end{bmatrix}. \quad (15)$$

Among them, $a_0 = 1$, $a_1 = -v$, and$a_2 = (-v) * (-v+1)/2$. It can be seen from the above 5*5 template that fractional orders of different orders have different processing effects.

In this paper, Matlab software is used to complete the programming of the fractional differential and perform image processing on the strong reflection image. By consulting the data, we can see that the Prewitt operator, the Sobel operator, the Laplacian operator, and the fractional differential algorithm all have the effect of reducing the influence of the strong reflection area and preserving the edge. Therefore, in image processing, this paper uses the above four algorithms to process the strong reflection area, and the image shown in Figure 6 is obtained.

As shown in Figure 6, it can be seen that although the Prewitt and Sobel operators perform better shadow processing on the reflective area, they have poor edge retention and are not suitable for future edge extraction. Although the Laplacian operator enhances the edge, the strong reflection area is not handled well, which produces a lot of false edges and affects the edge extraction. Fractional differentiation reduces the influence of the reflection area and preserves the edge information, which basically meets the requirements of this paper.

It can be seen from Figure 6(d) that the 0.3-order fractional differential has a good weakening of the strong reflection area, but there is still adhesion between the strong reflection area and the edge of the circular hole, which may also affect the edge extraction. Therefore, this paper decided to use different orders to process the image again to observe the effect. In this paper, the fractional differential when $v = 0.3$, 0.5, 0.7, and 0.8 is used to process the strong reflection area around the round hole of the artwork, and the image shown in Figure 7 is obtained.

It can be seen from the above figure that, as the order becomes larger, the effect of fractional differential on the high-brightness area of the strong reflection area is getting better and better, and the impact of the high-reflection area is getting smaller and smaller. Although the overall brightness of the image becomes darker as the order becomes larger, the preservation of the edge of the circular hole by the fractional differential is still very clear. Therefore, considering the two conditions of eliminating the influence of strong reflection area and edge retention, when the order $v = 0.8$, the processing effect is the best, so the image processed when $v = 0.8$ is used for edge extraction.

4. Experimental Analysis of Art Online Design System Based on Digital Simulation Technology

This study designs an art online design system based on digital simulation technology, as shown in Figure 8.

After constructing an art online design system based on digital simulation technology, the performance of the system is verified. This paper uses the intelligent system constructed in this paper to conduct multiple sets of simulation experiments to evaluate the digital effect and artistic design effect of the system constructed in this paper, and the results shown in Table 1 and Figure 9 are obtained.

From the above chart, the art online design system based on digital simulation technology designed in this paper basically meets the expected goals of the system designed in this paper and can improve the effect of art online design.

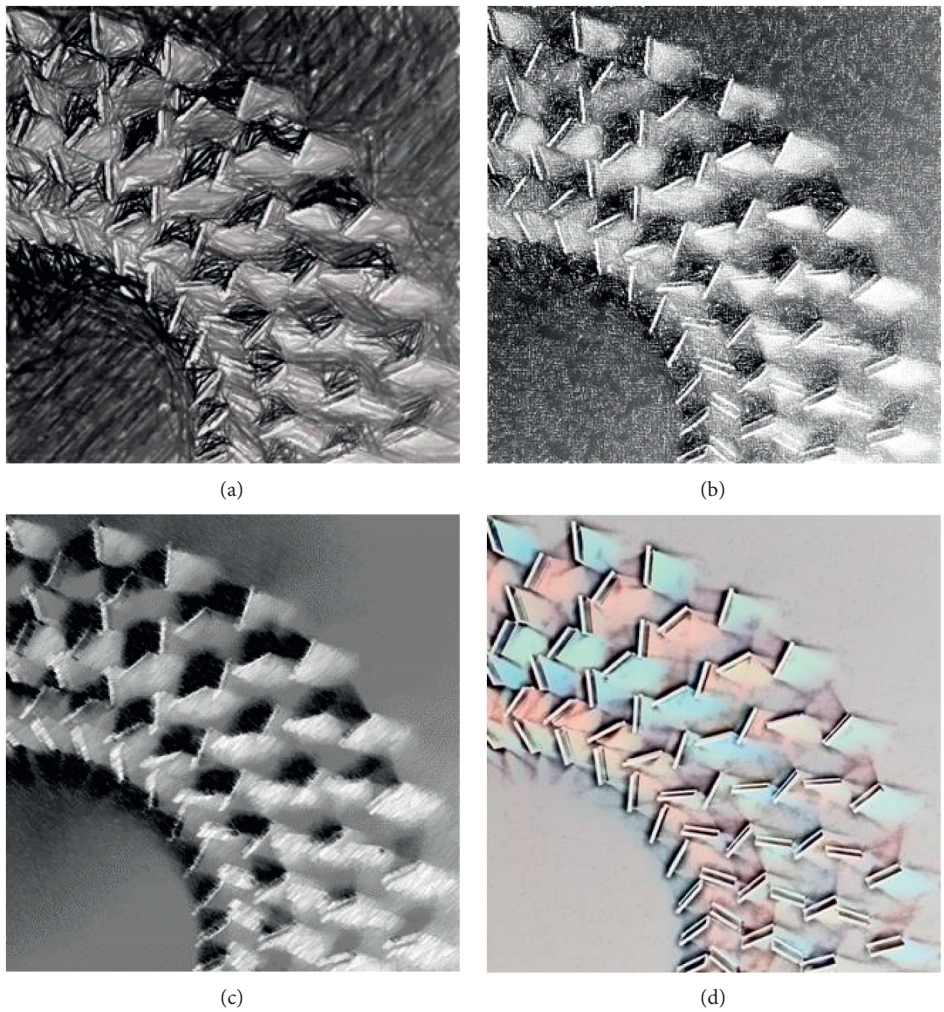

(a) (b)

(c) (d)

Figure 6: Processing of reflective images by different operators. (a) Prewitt operator. (b) Sobel operator. (c) Laplacian operator. (d) 0.3-order fractional differential.

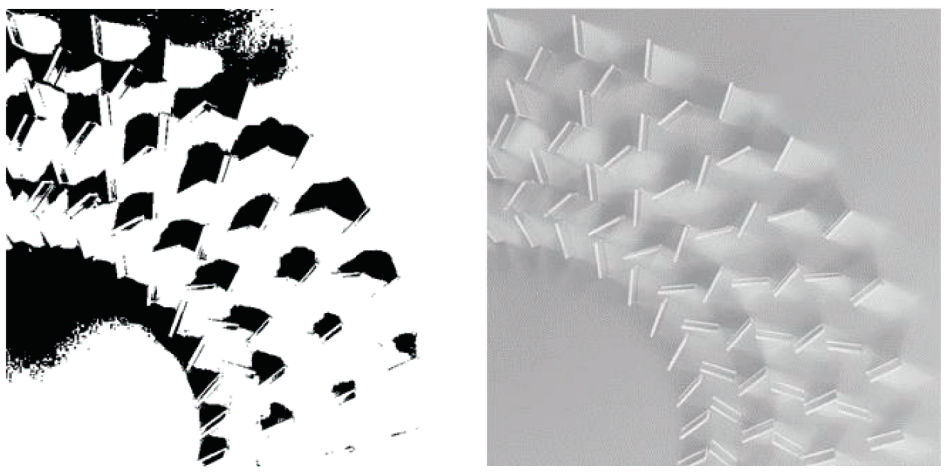

(a) (b)

Figure 7: Continued.

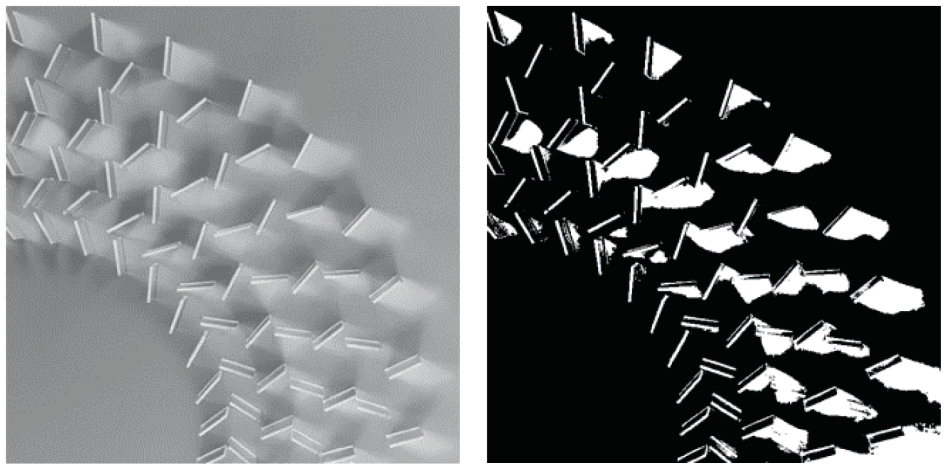

(c) (d)

Figure 7: Different order fractional differential processing image. (a) 0.3-order fractional differential. (b) 0.5-order fractional differential. (c) 0.7-order fractional differential. (d) 0.8-order fractional differential.

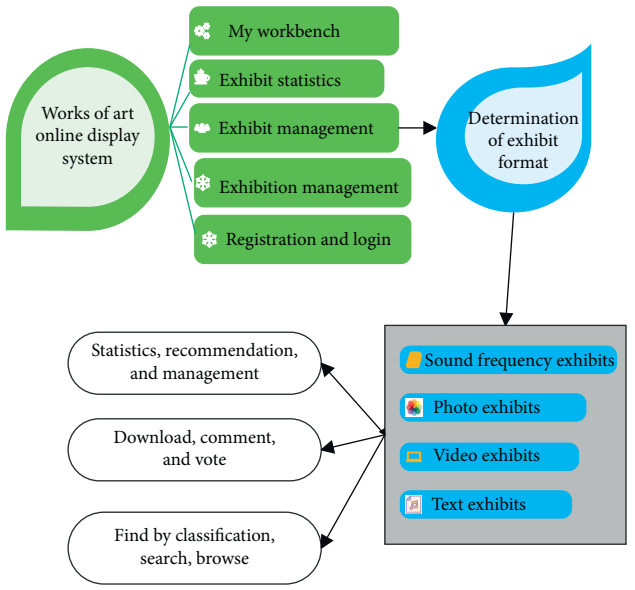

Figure 8: Art online design system based on digital simulation technology.

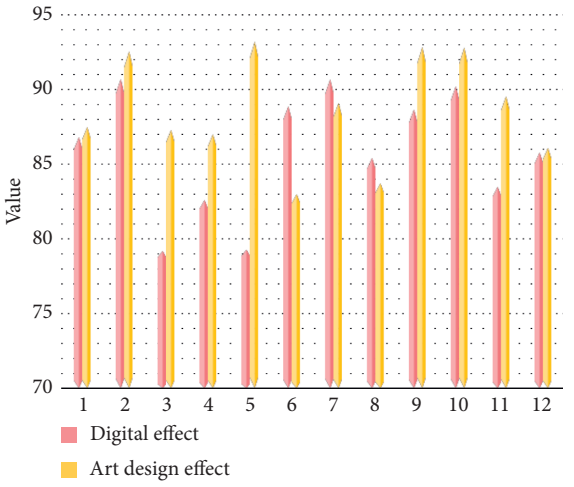

Figure 9: Histogram of experimental parameters of the art design system.

Table 1: System performance test results.

	Digital effect	Art design effect
1	86.80	87.49
2	90.69	92.55
3	79.20	87.29
4	82.60	87.00
5	79.29	93.20
6	88.87	82.99
7	90.67	89.09
8	85.42	83.72
9	88.65	92.83
10	90.21	92.80
11	83.48	89.54
12	85.78	86.09

5. Conclusion

With the development of Internet communication technology, the Internet disseminates information that everyone needs to Internet users in various forms such as texts, pictures, videos, and animations. However, due to the current hardware limitations such as network bandwidth and network traffic, it affects the speed of everyone's access to these media. At this time, streaming media as a new media application technology has solved this problem well. This article combines digital simulation technology to construct an art online design system. After constructing an art online design system based on digital simulation technology, the performance of the system is verified. Finally, this paper uses the intelligent system constructed in this paper to conduct multiple sets of simulation experiments to evaluate the digital effect and artistic design effect of the system constructed in this paper. From the experimental research, it can

be known that the art online design system based on digital simulation technology constructed in this paper basically meets the expected goals of the system constructed in this paper.

Data Availability

No datasets were generated or analyzed during the current study.

Conflicts of Interest

The author declares no conflicts of interest.

Acknowledgments

This work was supported by Xinyang Vocational and Technical College.

References

[1] N. McCartney and J. Tynan, "Fashioning contemporary art: a new interdisciplinary aesthetics in art-design collaborations," *Journal of Visual Art Practice*, vol. 20, no. 1-2, pp. 143–162, 2021.

[2] J. Lockheart, "The importance of writing as a material practice for art and design students: a contemporary rereading of the coldstream reports," *Art, Design & Communication in Higher Education*, vol. 17, no. 2, pp. 151–175, 2018.

[3] G. Sachdev, "Engaging with plants in an urban environment through street art and design," *Plants, People, Planet*, vol. 1, no. 3, pp. 271–289, 2019.

[4] Y. M. Andreeva, V. C. Luong, D. S. Lutoshina et al., "Laser coloration of metals in visual art and design," *Optical Materials Express*, vol. 9, no. 3, pp. 1310–1319, 2019.

[5] Z. Nebessayeva, K. Bekbolatova, K. Mussakulov, S. Zhanbirshiyev, and L. Tulepov, "Promotion of entrepreneurship development by art and design by pedagogy," *Opción*, vol. 34, no. 85-2, pp. 729–751, 2018.

[6] D. Mourtzis, "Simulation in the design and operation of manufacturing systems: state of the art and new trends," *International Journal of Production Research*, vol. 58, no. 7, pp. 1927–1949, 2020.

[7] K. W. Klockars, N. E. Yau, B. L. Tardy et al., "Asymmetrical coffee rings from cellulose nanocrystals and prospects in art and design," *Cellulose*, vol. 26, no. 1, pp. 491–506, 2019.

[8] M. Hermus, A. van Buuren, and V. Bekkers, "Applying design in public administration: a literature review to explore the state of the art," *Policy & Politics*, vol. 48, no. 1, pp. 21–48, 2020.

[9] J. Calvert and P. Schyfter, "What can science and technology studies learn from art and design? Reflections on 'synthetic aesthetics'," *Social Studies of Science*, vol. 47, no. 2, pp. 195–215, 2017.

[10] J. A. Greene, R. Freed, and R. K. Sawyer, "Fostering creative performance in art and design education via self-regulated learning," *Instructional Science*, vol. 47, no. 2, pp. 127–149, 2019.

[11] B. Bafandeh Mayvan, A. Rasoolzadegan, and Z. Ghavidel Yazdi, "The state of the art on design patterns: a systematic mapping of the literature," *Journal of Systems and Software*, vol. 125, no. C, pp. 93–118, 2017.

[12] A. Thorpe and E. Manzini, "Weaving people and places: art and design for resilient communities," *She Ji: The Journal of Design, Economics, and Innovation*, vol. 4, no. 1, pp. 1–10, 2018.

[13] M. Sclater and V. Lally, "Interdisciplinarity and technology-enhanced learning: reflections from art and design and educational perspectives," *Research in Comparative and International Education*, vol. 13, no. 1, pp. 46–69, 2018.

[14] V. Kinsella, "The use of activity theory as a methodology for developing creativity within the art and design classroom," *International Journal of Art & Design Education*, vol. 37, no. 3, pp. 493–506, 2018.

[15] C. Liu, S. Chen, C. Sheng, P. Ding, Z. Qian, and L. Ren, "The art of a hydraulic joint in a spider's leg: modelling, computational fluid dynamics (CFD) simulation, and bio-inspired design," *Journal of Comparative Physiology A*, vol. 205, no. 4, pp. 491–504, 2019.

[16] Z. Luo and J. Dai, "Synthetic genomics: the art of design and synthesis," *Chinese Journal of Biotechnology*, vol. 33, no. 3, pp. 331–342, 2017.

[17] E. Knight, J. Daymond, and S. Paroutis, "Design-led strategy: how to bring design thinking into the art of strategic management," *California Management Review*, vol. 62, no. 2, pp. 30–52, 2020.

[18] D. Jordan and H. O'Donoghue, "Histories of change in art and design education in Ireland: towards reform: the evolving trajectory of art education," *International Journal of Art & Design Education*, vol. 37, no. 4, pp. 574–586, 2018.

[19] T. Bastogne, "Quality-by-design of nanopharmaceuticals - a state of the art," *Nanomedicine: Nanotechnology, Biology and Medicine*, vol. 13, no. 7, pp. 2151–2157, 2017.

[20] K. Maras, "A realist account of critical agency in art criticism in art and design education," *International Journal of Art & Design Education*, vol. 37, no. 4, pp. 599–610, 2018.

[21] M. S. Ravelomanantsoa, Y. Ducq, and B. Vallespir, "A state of the art and comparison of approaches for performance measurement systems definition and design," *International Journal of Production Research*, vol. 57, no. 15-16, pp. 5026–5046, 2019.

[22] K. C. Tsai, "Teacher-student relationships, satisfaction, and achievement among art and design College students in Macau," *Journal of Education and Practice*, vol. 8, no. 6, pp. 12–16, 2017.